

Research Article

Cite this article: Castañeda-Quezada R, García-Mendoza E, Ramírez-Mendoza R, Helenes J, Rivas D, Romo-Curiel AE, Lago-Lestón A (2021). Distribution of *Gymnodinium catenatum* Graham cysts and its relation to harmful algae blooms in the northern Gulf of California. *Journal of the Marine Biological Association of the United Kingdom* **101**, 895–909. <https://doi.org/10.1017/S0025315421000795>

Received: 8 April 2021

Revised: 25 October 2021

Accepted: 29 October 2021

First published online: 8 December 2021








Key words:

Circulation patterns; cyst relocation;
Gymnodinium catenatum; HAB; PSP; seedbeds

Author for correspondence:

Ernesto García-Mendoza,
E-mail: ergarcia@cicese.mx

Distribution of *Gymnodinium catenatum* Graham cysts and its relation to harmful algae blooms in the northern Gulf of California

Rigel Castañeda-Quezada¹ , Ernesto García-Mendoza² , Rafael Ramírez-Mendoza³ , Javier Helenes⁴ , David Rivas² , Alfonsina E. Romo-Curiel² , and Asunción Lago-Lestón⁵ 

¹Posgrado de Ecología Marina, Centro de Investigación Científica y de Educación Superior de Ensenada, Carr. Ensenada-Tijuana #3918, CP 22860, Ensenada, Baja California, México; ²Departamento de Oceanografía Biológica, Centro de Investigación Científica y de Educación Superior de Ensenada, Carr. Ensenada-Tijuana #3918, CP 22860, Ensenada, Baja California, México; ³Departamento de Oceanografía Física, Centro de Investigación Científica y de Educación Superior de Ensenada, Carr. Ensenada-Tijuana, #3918, CP 22860, Ensenada, Baja California, México; ⁴Departamento de Geología, Centro de Investigación Científica y de Educación Superior de Ensenada, Carr. Ensenada-Tijuana, #3918, CP 22860, Ensenada, Baja California, México; and ⁵Departamento de Innovación Biomédica, Centro de Investigación Científica y de Educación Superior de Ensenada, Carr. Ensenada-Tijuana, #3918, CP 22860, Ensenada, Baja California, México

Abstract

Germination of cysts serves as inoculum for the proliferation of some dinoflagellates, and cyst abundance in sediments represents crucial information to understand and possibly predict Harmful Algae Blooms (HABs). Cyst distribution is related to the physical characteristics of the sediments and the hydrodynamics (circulation) of a particular region. In the northern Gulf of California (nGC) several *Gymnodinium catenatum* HABs have been recorded. However, the presence of resting cysts and the effect of hydrodynamics on their distribution in the nGC have not been investigated. This study evaluated cyst abundance, distribution and their relation to local circulation in surface sediments during two periods that coincided with a non-bloom year condition (July 2016) and after a major HAB registered in the nGC that occurred in January 2017. Also, a numerical ocean model was implemented to characterize the transport and relocation of cysts and sediments in the region. *Gymnodinium catenatum* cysts were heterogeneously distributed with some areas of high accumulation (as high as 158 cyst g⁻¹, and 27% of total cyst registered). Cysts seemed to be transported in an eastward direction after deposition and accumulated in an extensive area that probably is the seedbed responsible for the initiation of HABs in the region. The nGC is a retention area of cysts (and sediments) that permit the formation of seedbeds that could be important for *G. catenatum* HAB development. Our results provide key information to understand *G. catenatum* ecology and specifically, to understand the geographic and temporal appearance of HABs in the nGC.

Introduction

Ninety-five (65%) taxa of the ~147 species of marine microalgae associated with harmful algal blooms (HABs) are dinoflagellates, and they represent ~49% of the nearly 80 species identified as toxin producers (Peña *et al.*, 2016). Among the different toxins produced by dinoflagellates, paralytic shellfish toxins (PSTs) are of great concern, since these metabolites can cause mass mortalities of marine organisms and are transferred through the food chain to humans, representing a risk to public health.

PSTs are a group of at least 50 water-soluble neurotoxic alkaloid analogues to saxitoxin that are responsible for Paralytic Shellfish Poisoning (PSP) in humans (Wiese *et al.*, 2010). In the marine environment, PSTs are produced by *Gymnodinium catenatum*, *Pyrodinium bahamense* and different species of the genus *Alexandrium* (Band-Schmidt *et al.*, 2005; Penna *et al.*, 2015). Human fatalities have been associated with PSTs produced by *G. catenatum* (37 intoxicated and three deaths) and *P. bahamense* (476 intoxicated and 18 deaths) in Mexican Pacific coasts (Band-Schmidt *et al.*, 2019). *Gymnodinium catenatum* was described as a new species by Graham (1943) from samples collected during a cruise held in the Gulf of California (GC) in 1939. This species became notorious after an important PSP outbreak that occurred in 1979 in the coast of Sinaloa, Mexico when 18 people were intoxicated and three died after consuming bivalves contaminated with PSTs (Mee *et al.*, 1986). After this event, several *G. catenatum* proliferations have been recorded throughout the Pacific Mexican coast and in the GC but a negative impact has been documented in only a few of them (López-Cortés *et al.*, 2016; Medina-Elizalde *et al.*, 2018; Band-Schmidt *et al.*, 2019).

Gymnodinium catenatum HABs are a recurrent problem in the northern part of the GC (nGC). The presence of PSTs in this region affects fisheries, wildlife and has impacted public health. In 2010, the first sanitary ban was implemented in the nGC when PSTs concentrations in geoduck clams (*Panopea globosa*) were higher than the regulatory limit of 800 µg



STX eq kg⁻¹ (COFEPRIS, 2015). In the following years, no bans were implemented but in January 2015, PSTs concentrations in *P. globosa* reached up to 16,740 µg STX eq kg⁻¹ and the extraction of these organisms was prohibited for ~8 months (Medina-Elizalde *et al.*, 2018). Accumulation of PSTs in *P. globosa* was associated with a *G. catenatum* HAB that also caused mass mortalities of marine mammals and sea birds in the San Felipe region Medina-Elizalde (2021). Most importantly, five people were intoxicated in Los Angeles Bay after the consumption of unidentified clam species contaminated with PSTs (COFEPRIS, 2015). After 2015, HABs have occurred every year except for 2016 and have caused substantial economic losses due to the prohibition of the extraction of bivalves in the region (Medina-Elizalde, 2021).

The reason for the increase in the frequency of occurrence of *G. catenatum* HABs in the nGC is still unknown. Adequate environmental conditions must exist for cell proliferation but also a seeding population is needed for the development of *G. catenatum* HABs. Generation of temporal and resistance cysts is a strategy to cope with adverse conditions and facilitates the dispersion of *G. catenatum* (Dale, 1983). Cysts play a critical function in the reproduction of this species, and in other dinoflagellates (Figueroa & Bravo, 2005). Autochthonous and allochthonous *G. catenatum* bloom formation is associated with the location of the cyst beds in relation to where vegetative growth occurs (Hallegraeff *et al.*, 2012). In the first case, seedbeds with high concentrations of cysts are present in the same region (Tahvanainen *et al.*, 2012) where the proliferation of dinoflagellates occurs, as in the case of Tasmanian blooms. In allochthonous blooms, the abundance of *G. catenatum* cysts in surface sediments is insufficient for the generation of local HABs and seedbeds are located in nearby areas where excystment occurs (Hallegraeff *et al.*, 2012). For example, vegetative cells proliferate in the open ocean, and they are transported inshore. This type of HAB occurs in the coastal zone of the Atlantic Iberian Peninsula, specifically in the Galician Rias (Figueroa *et al.*, 2008).

Germination of cysts serves as an inoculum for the proliferation of some dinoflagellates, and cyst abundance in sediments represents crucial information to understand and possibly predict HABs (Erdner *et al.*, 2010). For example, recurrent HABs of *Alexandrium catenella* in the Gulf of Maine are closely related to local cyst seedbeds, and resuspension by currents and waves plays a critical role in cyst redistribution (Butman *et al.*, 2014). Physical stress and the erosion capacity of the sediment are related to the release and mobilization of cysts. Therefore, cyst distribution is related to physical characteristics of the sediments and the hydrodynamics of the region (Butman *et al.*, 2014). Cysts can behave as fine sediments since there is a high abundance of cysts in areas where this type of sediment dominates (Anderson *et al.*, 2005; Horner *et al.*, 2011; Triki *et al.*, 2017).

Gymnodinium catenatum HABs have been recently reported in the nGC (Gárate-Lizárraga *et al.*, 2007b; Medina-Elizalde *et al.*, 2018). The proliferations appear in a well-defined period from December/January to April/March (Ramírez Castillo, 2020) and they are probably associated with cyst seedbeds present in this region. However, there is no information about the presence of resting cysts of *G. catenatum* and the effect of hydrodynamics (circulation) on their distribution in the nGC. Therefore, we evaluated cyst abundance in surface sediments during two periods that coincided with a non-bloom year condition (July 2016) and after a major HAB registered in the nGC that occurred in January 2017. We related the distribution of the cysts to local circulation to characterize the transport and relocation of the cysts and sediments in the region. Our results provide key information to understand *G. catenatum* ecology and specifically, to understand the geographic and temporal appearance of HABs in the region.

Characteristics of the northern Gulf of California (nGC)

The Gulf of California has been divided into four zones according to their oceanographic, physical and biological conditions (Espinosa-Carreón & Valdez-Holguín, 2007). The present study was performed in the shallow (~200 m) northern Gulf of California (nGC) and the shallowest (~30 m) northernmost part denominated as the upper Gulf of California (uGC; Figure 1). The nGC presents a very well-defined seasonality with sea surface temperatures that reach 31–32 °C in August and September, while in January and February temperatures drop to 15–17 °C (Ramírez-León *et al.*, 2015). Specifically, the uGC is described as an inverse estuary (Lavín *et al.*, 1998) with an evaporation rate of 0.8 m y⁻¹ (Montes *et al.*, 2016). Salinity increases from 35.4 in open areas up to 39 in the shallow parts, due to low annual rainfall and the inverse estuarine conditions (Álvarez-Borrego *et al.*, 1975; Lavín *et al.*, 1998). Recorded currents reach 1 m s⁻¹ with tidal ranges up to 6 m (Argote *et al.*, 1995). Winds blow in a north-westerly direction from July to October, and cold and dry air blow in a south-easterly direction between December and May with speeds up to 8–12 m s⁻¹ cooling the surface waters in the Gulf (Bray & Robles, 1991).

Tidal amplitude increases in the uGC and the flow accumulates due to the narrowing and shallowing of the seafloor, increasing the maximum tidal range by ~10 m (Stock, 1976 in Brusca *et al.*, 2017). In the nGC the surface circulation presents a cyclonic gyre during summer (June–September) while an anticyclonic weak gyre occurs from November–March (Lavín *et al.*, 1997; Beier & Ripa, 1999; Palacios-Hernández *et al.*, 2002).

Materials and methods

Sample collection

Surface sediment samples (N = 53) were collected during two oceanographic campaigns (2016, 2017) on board the Tecolutla Research Vessel of the Mexican Navy. In 2016, a set of 25 samples was collected from 19–27 July. In the second campaign held from 23–28 February 2017, a total of 28 samples were collected. This second sampling period took place after one of the most major HABs in this region. The sampling stations were located between 30°–32°N and 112°–115°W at depths from 3–168 m (Figure 1).

Sediment samples were taken using a Mini Multi-Corer MC-200-4 from Ocean Instruments, Inc. It carries four 6.25 cm × 32.5 cm sample tubes with an effective penetration of 20 cm. Each sediment sample was stored in airtight containers in darkness at 4 °C until analysed in the laboratory.

Palynological analysis

Surface subsamples were lyophilized and processed by the modified palynomorph extraction technique of Wood *et al.* (1996). This technique consists in washing 10 g of freeze-dried sediment sample with detergent and adding a tablet of *Lycopodium clavatum* (Batch: 124,961 = 12,542 ± 931 spores per tablet; Lund University, Sweden) to estimate the concentration of cysts recovered per gram of dry sediment (cyst g⁻¹) (Maher, 1981; Mertens *et al.*, 2009, 2012). The carbonate elements and silicates were removed with hydrochloric acid and hydrofluoric acid, respectively. After this treatment, sodium polytungstate (Density = 2) was added to separate organic and inorganic matter and sieved to isolate the 120–15 µm fraction. Finally, 7–10 drops of the residue were collected and mounted on a 25 × 50 mm coverslip with glycerine-jelly. The cyst concentrations for the 53 samples were calculated using the Benninghoff's (1962) formula. The mean and standard deviation were calculated for the exotic marker (*Lycopodium*) recovered from all samples (Maher, 1981).

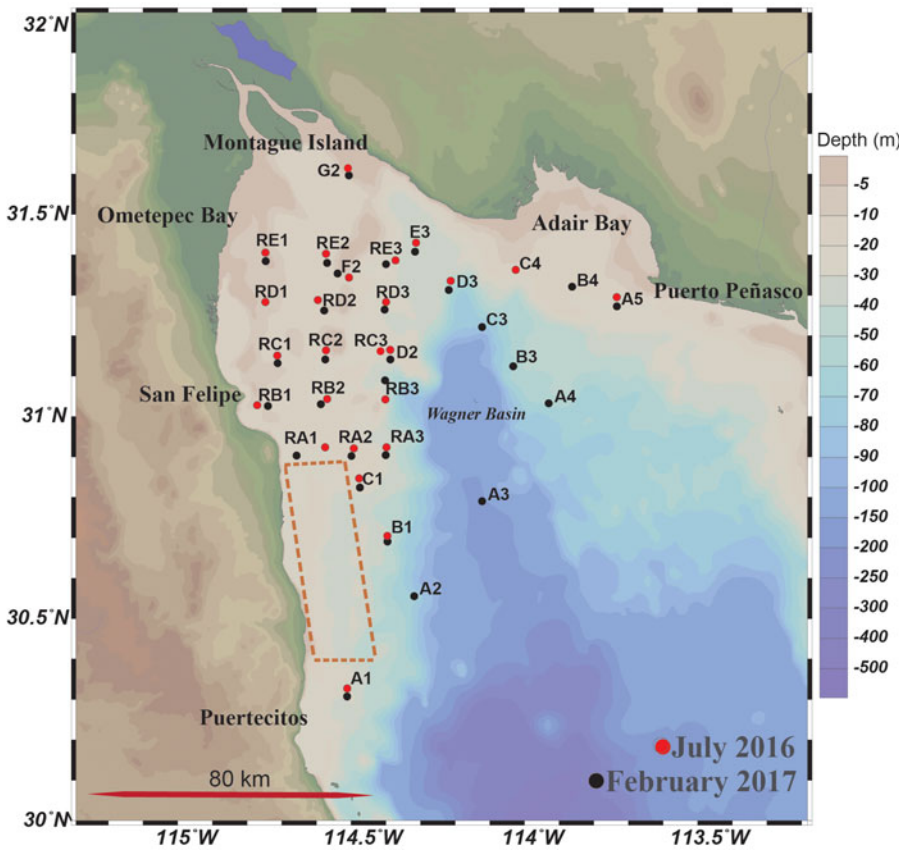


Fig. 1. Northern (nGC) and upper Gulf of California (uGC), and sample collection during July 2016 (red dots; N=25) and February 2017 (black dots; N=28). *Panopea globosa* extraction area is highlighted in a dashed red line.

Considering the low recovery of organic-walled dinoflagellate cysts, a minimum sample size (n_0) was calculated based on values of *L. clavatum* spores ($N = 12,542$) as a finite population. Cochran’s Formula ($n_0 = Z^2 p q / e^2$) (Cochran, 1963; Singh & Masuku, 2013) was applied with a confidence of 95% ($Z = 1.96$) and a margin of error of 5% ($e = 0.05$). As a result, a minimum expected number of *L. clavatum* was 412-spores for tablets with 12,542-spores and a standard deviation in *L. clavatum* recovery of 804 spores in the 53 samples. Therefore, this study considered the presence of at least 800 spores in the palynological laminae recovery. The plates were analysed (duplicate) with an Olympus optical microscope (CX31) at $400\times$ magnification, and sweeps were made from one side to the other of the plates, completely covering the surface with ~ 24 sweeps. For a more detailed analysis of the cysts present in the samples $600\times$ and $1000\times$ amplifications were used. Photographs were taken with an Olympus camera integrated to the microscope. *Gymnodinium catenatum* cysts were identified according to their size, shape and reticulation as described by Anderson *et al.* (1988), Rees & Hallegraeff (1991) and Bolch *et al.* (1999). The abundance of *G. catenatum* cysts found in the samples were quantified to determine their contribution to the trophic affinity of dinoflagellate cysts of other species found in the samples.

Granulometry analysis

The sediment in the study area is predominantly silt, clay and fine sand (Carriquiry *et al.*, 2001). To characterize the type of sediments present in the study area a subsample was wetly sieved ($350\text{--}500\ \mu\text{m}$). The fine portion that passed through the sieves was gauged with distilled water and sodium oxalate was added as a dispersant, and the mixture was agitated. A subsample was diluted with distilled water and sodium oxalate, shaken and added to the analysis chamber of the LISST model 100X-C Laser In-Situ Scattering and Transmissometer (LISST-100X –

Sequoia Scientific). The angular range programmed in the Transmissometer corresponds to a spherical particle size range of $2.5\text{--}500\ \mu\text{m}$ diameter. The grain size distribution was estimated with the GRADISTAT v8.0 software (Blott & Pye, 2001). The Udden–Wentworth granulometric scale was used to classify the type of sediment present in the samples (Wentworth, 1922) (Table S2).

Chlorophyll-a satellite analysis

Satellite chlorophyll-a (Chl_{sat}) images were obtained from the Sentinel-3 OLCI Level 2 full resolution (WFR). Chlorophyll-a concentration values were extracted for 28 stations (Table S3), with a spatial resolution of 300 m per pixel for different dates of 2017 when images were available (6, 18, 19, 30 January, 10, 21, 25 February and 1 March). Products were directly obtained from the Copernicus Online Data Access (CODA) of the European Space Agency (ESA) and processed with SNAP-ESA Sentinel Application Platform v7.0.0 (<http://step.esa.int>).

A monitoring program for *G. catenatum* has been conducted by FICOTOX laboratory (CICESE) since 2011 in the *P. globosa* clam extraction areas located south of San Felipe (Figure 1). The database was consulted for surface cell abundance reported in cells l^{-1} , thus the information for abundance is limited to this area.

Statistical analysis

The distribution of cyst concentrations from the 53 sampling stations were tested for normality with a Shapiro–Wilk test. Data distribution failed the normality test, and differences in *G. catenatum* cyst concentrations by years were tested with a Wilcoxon test, comparing paired samples and considering increases or decreases in the concentrations, also the number of

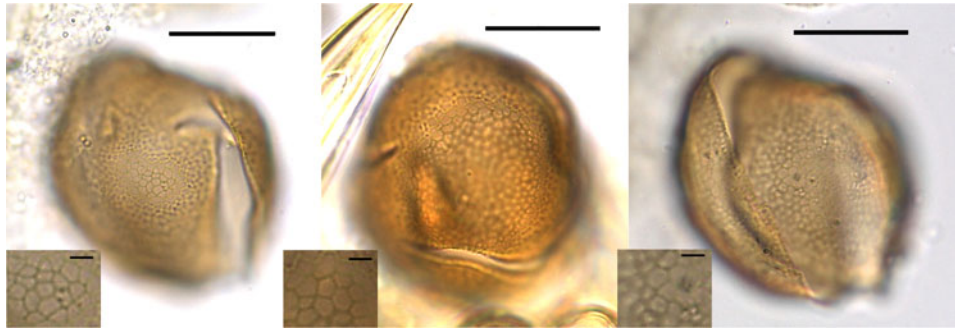


Fig. 2. *Gymnodinium catenatum* cysts found in sediments collected in the northern Gulf of California. The reticulate delineate five to six-sided paravesicles (details in lower left corner of the photographs, scale bar 2 μm). The empty cysts are divided roughly in half. Scale bar 20 μm .

both negative and positive differences were analysed (Siegel & Castellan, 1988).

A principal component analysis (PCA) was performed to evaluate the relationship between satellite derived Chl_{sat} and the abundance of cysts in the nGC. PCA was applied to simplify the complexity in the relationship between the distribution and abundance of *G. catenatum* cysts, and the Chl_{sat} values in the 28 stations sampled in February 2017. The level of significance of all statistical tests was $\alpha = 0.05$. Analyses were performed with Statistica software v12.5 (StatSoft, 2014).

The association between the sediment grain size and *G. catenatum* cyst concentrations was also verified on both sampling years with cluster analysis. The Unweighted pair-group average (UPGMA) algorithm using the correlation distance matrix of the sediment component (in %) and cyst concentration in the nGC by year was used to explore the association between variables. These analyses were performed in the software PAST v4.02 (Hammer *et al.*, 2001).

Cyst geographic distribution analysis

Gymnodinium catenatum cyst concentrations interpolation between stations was performed with the Data-Interpolating Variational Analysis tool (DIVA) of Ocean Data View (ODV v5.5.1) software (Schlitzer, 2021). Cyst distribution was compared with the mean surface currents velocity field at 5 m above the bottom for July 2016 and February 2017. These velocity fields were generated with a Numerical Ocean Model implemented in the region.

Numerical Ocean Model and particle-tracking experiments

Numerical ocean-model outputs were included in the analysis to elucidate the possible origin and distribution of the cysts in the nGC. This numerical model is based on the Regional Ocean Modeling System (ROMS, e.g. Rivas & Samelson, 2011). It extends from the nGC through ~ 500 km beyond the Gulf's mouth (see Figure S1). The model has a horizontal resolution of ~ 3 km and 22 sigma levels in the vertical (with enhanced resolution near the bottom and the surface). The configuration, mixing/advection schemes and boundary treatment are based on the regional model used by Cruz-Rico & Rivas (2018). Monthly data from the Global Ocean Data Assimilation System (GODAS; e.g. Ravichandran *et al.*, 2013) were used in the model's lateral open boundaries, adding daily sea surface height and geostrophic velocity taken from an altimeter gridded product of absolute dynamic topography (Rio *et al.*, 2014). At the surface, net heat flux, freshwater flux (evaporation minus precipitation), and wind stress were calculated internally in the model, using bulk formulae (Fairall *et al.*, 1996), from meteorological surface fields

from the North American Regional Reanalysis (NARR; Mesinger *et al.*, 2006).

In particular for the nGC, a comparison between monthly sea surface temperature of the model and the corresponding satellite product shows high correlations ($r \geq 0.94$) for the 2013–2017 period, and moderate correlations ($0.40 \leq r_{\text{an}} \leq 0.79$) after removing the mean seasonal cycle (Figure S1). The lowest correlations are found in a small northern area, most probably associated with a water input from land, which is absent in the model. Although a comparison with other variables such as water velocity is necessary to determine if the model reproduces the water circulation adequately, as will be shown below, the model shows circulation patterns consistent with those reported in the literature, which reinforces the confidence in this numerically modelled velocity field.

Geographic origin of the cysts found in the uGC was explored by a Lagrangian particle-tracking method based on Rivas & Samelson (2011). This approach consists of computing paths of particles that are passively advected by the model's three-dimensional velocity field. Groups of particles were initialized at the positions of the observational points and advected backward in time for 30 days (analysing intermediate points at 6, 14, 22 and 30 days), to determine the possible locations of the sources of cysts assuming that they were generated by vegetative cells during the HAB. In this way, the image of the Lagrangian paths during the 22 days prior to the particles release was selected in both analyses (July and February) since the particles manage to separate sufficiently from their initial point without leaving the domain determined in the analysis (Figure S2).

For analysis of the July-2016 sampling period, particles were released on 22 July at bottom depth for the 20 observational points with non-zero cyst concentration. Similarly, for the February-2017 analysis, particles were released on 25 February at the surface of the 23 observational points with non-zero cyst concentration. The objective of these experiments was to explain the possible origin of the cysts of *G. catenatum* observed in July 2016 and February 2017 by taking as a destination the location at the time of sampling.

Results

Gymnodinium catenatum cysts were pale brown, spherical and microreticulated (five and six-sided), with low (< 2 μm) rounded ridges that covered the entire cyst surface (Figure 2). The diameter of the cysts collected in the nGC ranged from 38–60 μm . The cingulum was bordered by two cingular bands, and the sulcus presented a longitudinal line of paravesicles that begins at the lower margin of the flagellar pore region, showing a whorled pattern of paravesicles. Cysts were often split along the edge of the cingulum (roughly in half) as described by Anderson *et al.* (1988) (Figure 2).

Cysts of *G. catenatum* were identified in 43 of the 53 sampling locations ($N = 20$ in 2016, $N = 23$ in 2017). In July 2016, *G. catenatum* represented 23% (805 cysts) of the assemblage of 3481 cysts, and 39% of the autotrophic species cysts. In February 2017, the relative abundance of *G. catenatum* increased slightly to 27% (1146 cysts) of the total cyst assemblage (4223), where autotrophic species represented 51%. Cyst assemblages in surface sediments of the nGC showed a high diversity with respect to the GC.

Cyst concentrations in sediments observed in 2016 ($N = 805$) were significantly different to the ones detected in 2017 ($N = 1146$, $P = 0.021$). In 2016, concentrations varied between 6–124 cyst g^{-1} with an average of 32 cyst g^{-1} and in 2017, concentrations varied from 8–158 cyst g^{-1} (41 cyst g^{-1} ; Table S1). In general, during both sampling years the same relative abundance of empty cysts (~50–60%) was observed, except in those stations located close to Adair Bay where all the cysts were open in 2017.

Cyst geographic distribution

The geographic distribution of the cysts and their relationship with the bathymetry was analysed to characterize areas that presented a change in cyst accumulation between sampling periods.

The sampling effort was concentrated on relatively shallow stations. Only a few sampling stations were in depths below 50 m. Most of the *G. catenatum* cyst found in July 2016 (92%) were distributed in a range between 3–32 m depth (Figure 3A). The remaining 8% of the cysts were present in sediments below 42 m depth (Figure 3A). In February 2017, 85% of the cysts were accumulated in the range between 3–32 m depth. In this period (Figure 3B), some samples were collected in depths below 50 m. 61 cyst g^{-1} were registered at 67 m in station B3, and 7 cyst g^{-1} were detected in a sample collected from the Consag Basin at a depth of 168 m (Figure 3B). Therefore, the major proportion of *G. catenatum* cysts were found above 30 m depth in the shallow zone of the nGC. They were heterogeneously distributed in this area. In 2016, cysts were present in the north and north-east zones, and mainly constrained to the uGC (Figure 3C). A clear accumulation area with cyst concentrations of 110–120 cyst g^{-1} was located off the coast between San Felipe and Ometepec Bay extending north-north-east towards the coast of Sonora (Figure 3C). A different distribution pattern was observed in 2017. Three accumulation areas with high cyst concentrations were identified: (1) the west coast of the southern nGC between San Felipe and Puertecitos with concentrations higher than 150 cyst g^{-1} ; (2) the Adair Bay at the north-west of Puerto Peñasco with 112 cyst g^{-1} ; and (3) south of Montague Island in the centre of the uGC in the Colorado River Delta Biosphere Reserve with concentrations around 90 cyst g^{-1} (Figure 3D).

Granulometry characteristics of the sediment

The analysis of the type of sediment present in the nGC during the 2016 and 2017 sampling campaigns was performed to evaluate if cysts were associated with specific sediment types and if they presented a similar spatial distribution pattern. The sediment grain composition was similar in both sampling periods (Table 1). Silts (≈ 2 –63 μm) represented 79.3 and 74.6% of all grain components for July 2016 and February 2017, respectively. Sands represented 20.6% of all grain fractions for July 2016 and 25.3% in February 2017. In July 2016 clay represented 1.4% of all components and was absent in February 2017. Representation of the sand subfractions was also similar in both sampling periods, with the exception of medium sand that was 0.3% of all sediment components in July 2017 and 6.3% in February 2017. In relation to mud subfractions, fine and very

fine silts were more represented (20.4 and 12.5%) in July 2016 than in February 2017 samples (9.9 and 1.2%; Table 1 and Table 2S).

We analysed the relation between the type of sediment and the presence of *G. catenatum* cysts in each station of both sampling campaigns. *Gymnodinium catenatum* cysts were associated with different sediment components in the two sampling periods. In February 2017, *G. catenatum* and the fine sand fraction formed a group that was separated from the rest of the granulometric components with a similarity value of 0.2. In contrast, in July 2016 cysts were associated with fine silt (corr. 0.3), a much smaller size fraction component. The association of fine silt and fine sand with the presence of *G. catenatum* cysts was evident when the spatial distribution of these sediment fractions was analysed. In July 2016 the highest accumulation of fine silt was found in front of San Felipe and Ometepec Bay (Figure 3E). This type of grain represented ~20% of the sediments and, as described before, a high concentration of *G. catenatum* cysts was also found in these areas (Figure 3C). In February 2017, similar to the *G. catenatum* cyst distribution, fine sands accumulated in two well-defined areas of the nGC. Fine sand represented ~8% of the sediment components close to the coast south from San Felipe to Puertecitos, and in front of Adair Bay, in the east coast of the region (Figure 3F).

Deposition of the cysts produced by *G. catenatum*, transport and relocation define the accumulation areas of this material. Sediments are also exposed to transportation and relocation processes. In February 2017 the geographic distribution of the cysts could be related to the HAB of *G. catenatum* that occurred one month before.

The 2017 *G. catenatum* HAB

Gymnodinium catenatum is commonly present in the *P. globosa* extraction areas from November/December to April/May (Medina-Elizalde *et al.*, 2018). In the 2015 HAB *G. catenatum* maximum surface cell abundance was 152×10^3 cells l^{-1} and represented as much as 55% of all species collected in net samples (Medina-Elizalde *et al.*, 2018). In 2016, maximum surface cell abundance in January was 320 cells l^{-1} ; therefore, cyst abundance detected in July of this year was associated with a non-bloom year. In contrast, cysts in February 2017 were associated with a bloom that occurred before the sampling period. *Gymnodinium catenatum* was detected from January (no samples were obtained in December) to May 2017 in the clam extraction areas. The highest abundance of 311×10^3 cells l^{-1} in surface was detected in January 17 (Figure 4) and *G. catenatum* represented 92% of the phytoplankton community on this date (Figure 4). Cell abundances decreased to 283×10^3 cells l^{-1} in January 23 and to 28.5×10^3 cells l^{-1} in February. On these dates, *G. catenatum* still was highly represented in net samples (higher than 60%) and detected in various samples collected in April but not in May (Figure 4).

Information of the HAB was limited to *P. globosa* extraction area. Therefore, to evaluate the probable extension and evolution of the HAB in the region, the distribution of the chlorophyll-*a* concentration was estimated from satellite data (Chl_{sat}). On 6 January, the accumulation of Chl_{sat} was evident as filaments in the west coast south from San Felipe Bay. On 18 and 19 January, the area of high Chl_{sat} increased in the west coast of the nGC. Especially, concentrations higher than 15 mg m^{-3} were detected in an area of $\sim 600 \text{ km}^2$ located parallel to the coast between San Felipe and Puertecitos. Low Chl_{sat} were present to the north and to the east of this area. Another Chl_{sat} accumulation area was detected in the continental coast of the nGC close to Adair Bay and Puerto Peñasco. The highest Chl_{sat} (23 mg m^{-3}) and the largest extension of the bloom were detected

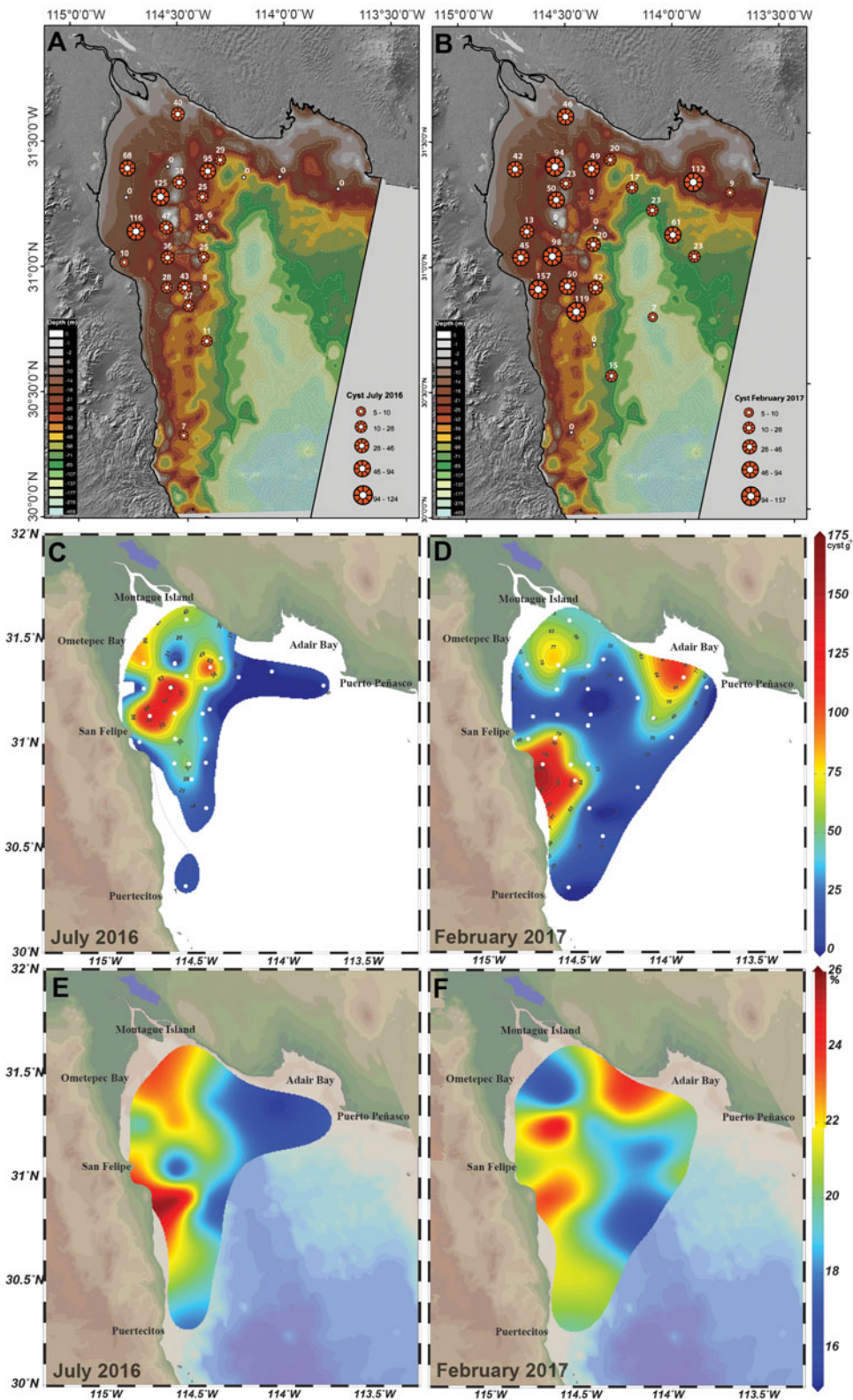


Fig. 3. Distribution of cysts in the northern Gulf of California, the image shows bathymetry and cyst concentration during (A) July 2016, and (B) February 2017 sampling campaigns. Geographic distribution of *G. catenatum* cysts concentrations observed during (C) July 2016 and (D) February 2017. Right scale shows concentrations from 0 to 175 cysts g^{-1} . (E) Distribution of fine silts (in %) in July 2016 and (F) fine sands (in %) in February 2017 in the northern Gulf of California.

on 10 February (Figure 5). During the period of the sampling campaign the Chl_{sat} decreased as seen in the images of 21, 25 February and 1 March (Figure 5). After this last date, Chl_{sat} was lower than 5 mg m^{-3} in the region. Chl_{sat} indicates that the bloom initiated in the west side of the Gulf south from San Felipe (although there is also a small area of high Chl_{sat} in the

continental side of the Gulf) and moved and dispersed in a northward but principally in a westward direction.

The result of the particle-tracking analysis, introduced in the Chl_{sat} maps, also indicates this dispersion pattern of the bloom. For example, particles of 19 January that originated in the west coast of the Gulf showed westward and northward trajectories

Table 1. Granulometric composition (in percentage) of sediment samples collected in July 2016 and February 2017 in the northern Gulf of California

	SAND	MUD	Medium sand	Fine sand	Very fine sand	Very coarse silt	Coarse silt	Medium silt	Fine silt	Very fine silt	Clay
July 2016	20.6	79.3	0.3	6	10.3	13.8	17.5	18.9	20.4	12.5	1.4
February 2017	25.3	74.6	6.3	8.2	10.7	17.9	18.1	20	9.9	1.2	0
Range (μm)			500–250	250–125	125–63	63–32	32–16	16–8	8–4	4–2	2–0.25

Micron size range is presented.

and remained in the nGC, mainly in the upper region (Figure 5). Therefore, the areas of high cysts accumulation in February 2017 were probably related to the appearance and dispersion of the HAB.

To probe this assumption, the relation between Chl_{sat} and cysts abundance in the sediment was analysed with a principal component analysis (PCA).

Three factors of the PCA explained 73.1% of the total variance of the relation between Chl_{sat} during different dates and *G. catenatum* cyst abundance (Table S4). PCA showed the formation of two groups. 6, 18, 30 January and 25 February, and 1 March 2017, formed a group with lower Chl_{sat} concentration compared with the second group comprising 19 January, 10 and 21 February, that was positively correlated with cyst abundance (Figure 6). This analysis supports the assumption that February 2017 seedbeds originated from the HAB present in the region ~1 month before the sampling period.

Cyst dynamics in the northern Gulf of California

Gymnodinium catenatum cyst distribution in February coincided with the distribution of relatively large grain types of sediments (fine sands) and of Chl_{sat} . Therefore, location of seedbeds in February was probably associated with the bloom of the dinoflagellate and its dispersion. To check this, we evaluated the dispersion of vegetative cells related to water circulation using a numerical circulation model and particle advection experiments. The circulation pattern at the surface and at 5 m above the bottom were characterized during February 2017 in the nGC (Figure 7A). Surface circulation in this month was dominated by a strong anticyclonic eddy located south of the sampling area at about 30.5° N. The highest speeds both on the surface and close to the bottom were present in this eddy with a maximum mean of 0.42 and 0.12 m s^{-1} , respectively. The intensity of surface currents decreased northward from the eddy where a west to the east flow direction was clearly evident around 31°N. As the intensity of surface currents decreased towards the northernmost part of the uGC, the circulation showed different directions. Especially south of Montague Island and south of San Felipe there was a poorly defined circulation pattern. In this region surface, current speeds were <0.10 m s^{-1} . In contrast to surface circulation, there was an unclear circulation pattern at the bottom of the uGC and, in general, the current speeds are slower than ones at the surface.

Cyst beds were found in locations with weak surface and bottom flow as was evident in the west and in the northern areas of the nGC. Also, a high cyst accumulation area was located where the surface direction of the flow was towards the coast, as in Adair Bay (Figure 7A). The location of the cysts for this period seemed to be unrelated to the near-bottom circulation. This was confirmed by the modelled Lagrangian particle-tracking results (Figure 7B).

We followed the movement of particles released on the surface assuming that the cysts found in the sediment originated from the HAB recorded during this period. The origin of the cysts located in areas of low concentration (<80 cysts g^{-1}) in the sediments was heterogeneous (Figure 7B 1). In contrast, cysts in high accumulation areas originated from nearby locations. The cysts in seedbeds detected between San Felipe and Puertecitos most probably had their origin in northern locations, then were transported in a southward direction (Figure 7B 2–4).

The cysts on the continental side of the nGC (Adair Bay) seemed to originate from particles (vegetative cells) located northwest and southward from this location and it is likely they are transported from the uGC towards Adair Bay. The cysts located close to Montague Island are related to particles present south from this location or seemed trapped in this area

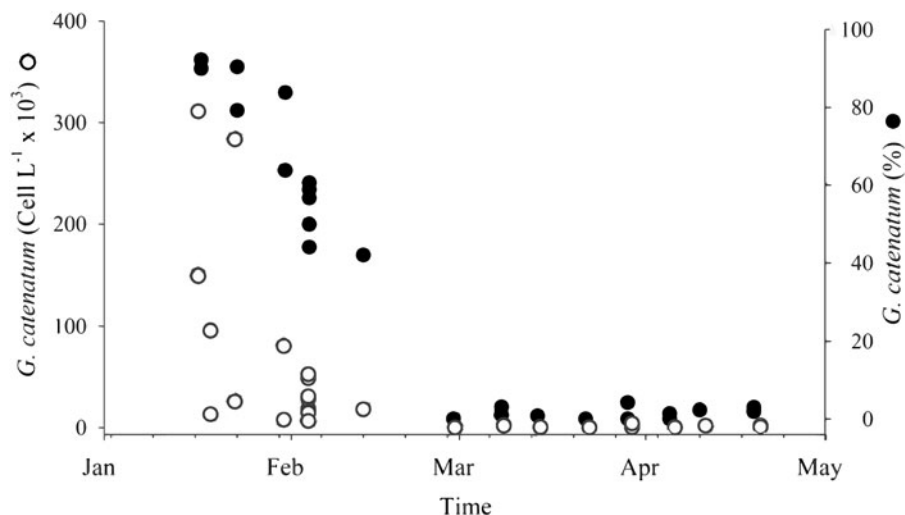


Fig. 4. *Gymnodinium catenatum* surface abundance and relative abundance in net samples collected in the clam extraction area south from San Felipe, B.C.

(Figure 7B1 and B3). Circulation and particle-tracking analysis indicate that HABs present a local behaviour since cysts are deposited during vegetative proliferation and remain trapped in the northern part of the region. This was corroborated in the analysis of the circulation condition and particle tracking during the cyclonic gyre in July 2016. In this period, the circulation is characterized by a strong cyclonic eddy centred around 30.5°N and strong surface currents on the east side oriented towards the uGC (white vectors in Figure 8A). The surface currents were more intense than the ones present in February 2017, since they reached speeds up to 0.54 ms^{-1} . Currents at the bottom were weaker (0.15 ms^{-1}) than surface currents. The strongest currents were present in the upper part of the Gulf and in the west coast related to the eddy located at 30.5°N . In both areas, the bottom circulation presented a southward direction. The high concentration of cysts of *G. catenatum* in the peninsular side of the uGC is most likely related to the bottom circulation pattern. Seedbed was located in an area where bottom speeds and direction were different from the surrounding predominant pattern. There is a strong east to west current in the northernmost part of the uGC that turns southward, and flows close to the coast (Figure 8A). The west cysts are retained since the speed of the bottom is minimal in this area and runs to the north-east direction (Figure 8A, B).

Particle tracking analysis indicates also that close to the bottom, hydrodynamics influenced sediment and cyst localization after being deposited by a HAB event in the nGC. At least, it is related to the localization of the seedbed during July 2016. In this period, particle surface movement was strongly influenced by the cyclonic circulation (Figure 8A). The origin of most of the 20 particles released in July 2016 was far south and outside of the surrounding area of the uGC (Figure 8B). The trajectories clearly follow surface circulation and do not correlate with the location of the seedbed. The particle-advection experiments for both periods (July 2016 and February 2017) confirm the effect of circulation on the distribution of *G. catenatum* cysts on the nGC.

Discussion

Gymnodinium catenatum cysts were present in recent sediments of the northern part of the Gulf of California. Cysts were heterogeneously distributed, and areas of high accumulation were detected. Seedbeds were dynamic since variation in cyst abundance and geographic distribution was evident during different seasons. Cysts of *G. catenatum* were highly represented in the sediments (as much as 27% of the total cysts) and presented a wide geographic distribution.

The representation of *G. catenatum* seems unusually high, since Pospelova et al. (2008) reported a relative abundance of 0.3% of this species in sediments collected close to the nGC. Also, the percentage found in the nGC seems atypical when compared with other regions (Table S5). *Gymnodinium catenatum* represented 3.1% of cyst assemblages from Concepcion Bay (Morquecho & Lechuga-Devéze, 2003), and 5.6% in Pescadero Basin (Duque-Herrera et al., 2020) within the GC. Cyst representation in the nGC is much higher than in the coasts of Korea (0.3–3%; Pospelova & Kim, 2010; Shin et al., 2011) and China (0.3–2.6%; Wang et al., 2004; Hwang et al., 2011; Liu et al., 2012), Swedish fjords (0.3%; Harland et al., 2004), Baltic Sea (0.6%; Nehring, 1994), Tasmania (3.4%; Bolch & Hallegraeff, 1990) and Lisbon Bay (5%, Ribeiro & Amorim, 2008). However, the percentage of *G. catenatum* cysts in the nGC is similar or lower than in other regions where recurrent HABs occur. *Gymnodinium catenatum* cysts along the Portuguese coast could represent $\sim 24\%$ of the cysts found in the sediments and can reach a representation as high as 71% (Amorim & Dale, 1998; Amorim et al., 2001). High concentrations are recorded after recurrent HABs events in different points of the Portuguese coast, being deposited from November to January and in mid-July (Amorim et al., 2001). In the coast of Galicia, specifically in Ria de Arousa, high concentrations of *G. catenatum* cysts have also been reported (Blanco, 1995). The high variability in the relative concentrations of cysts is probably related to the type of sampling and methodological approaches, but most importantly to the heterogeneous distribution and the presence of areas of high accumulation of *G. catenatum* cysts.

This is the only work where *G. catenatum* seedbeds are described in detail. In the areas with high accumulation of cysts the extension of seedbeds has not been characterized, nor the temporal variation of its abundance associated with the dynamics of these regions.

The seedbeds detected on February 2017 were related to a *G. catenatum* HAB that occurred during winter in the nGC. The presence of *G. catenatum* cysts related to recurrent HABs has been documented in other regions of the world but there is not a clear pattern between cyst concentration found in the sediment and vegetative cell abundance in the water column (Table S6). For example, the highest cyst abundance has been reported in the West Coast of the North Island in New Zealand after 2000 and 2001 HABs (MacKenzie, 2014). Maximum cyst concentration was $10,200\text{ cysts cm}^{-2}$ that was related to a maximum cell abundance of $27 \times 10^3\text{ cells l}^{-1}$ detected in the surf zone (MacKenzie, 2014). In contrast, only 40 cysts g^{-1} were

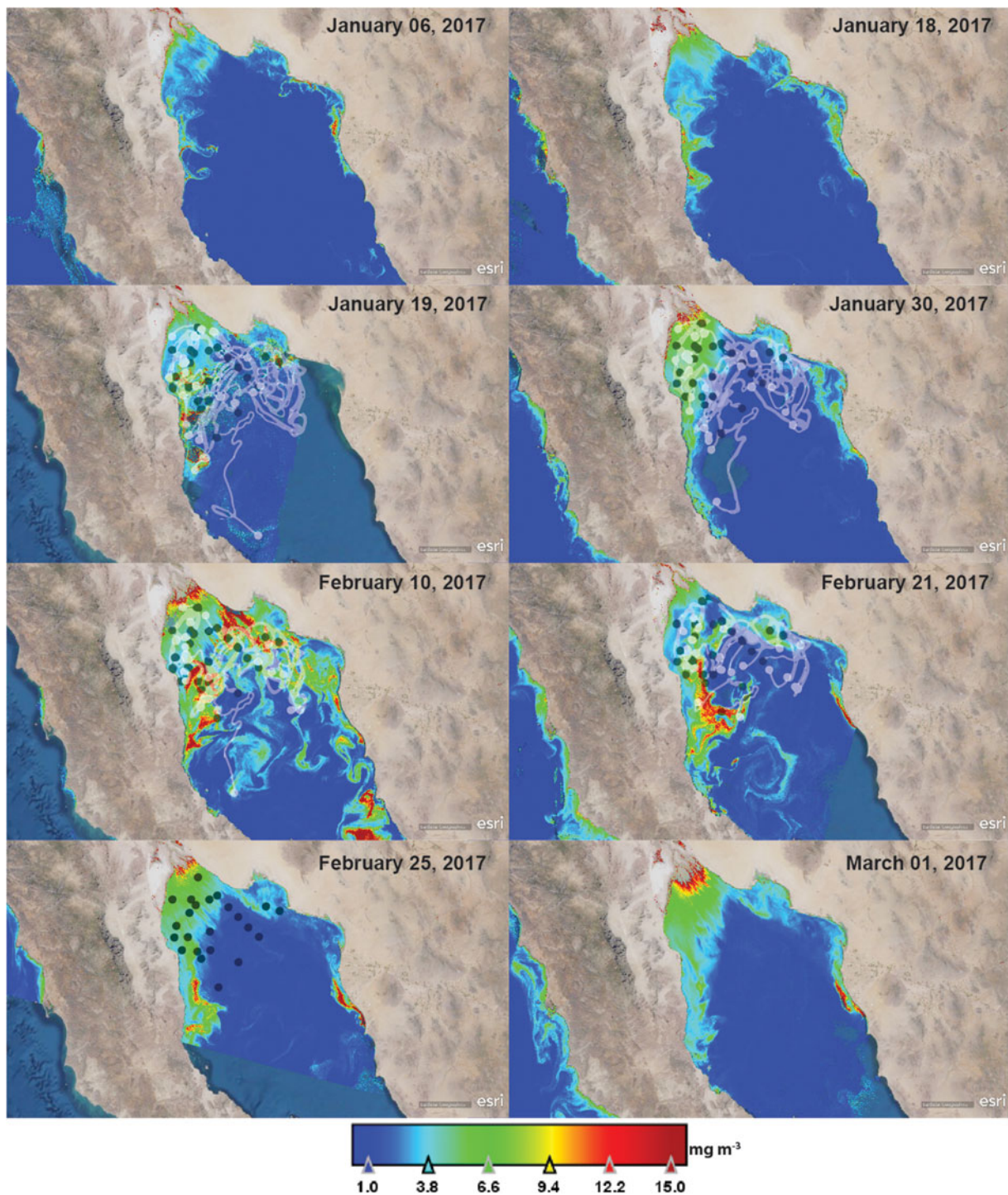


Fig. 5. Distribution of satellite-derived chlorophyll-*a* concentration (Chl_{sat}) in January and February 2017 in the northern Gulf of California. Chl_{sat} is presented at a maximum concentration of 15 mg m^{-3} in the figures. Lagrangian trajectories estimated from the Lagrangian particle-tracking analysis from 19 January to 25 February 2017 are also presented. Black dots represent the final position of the advected particles on 25 February. The white dots represent the position of the particles in the daytime indicated on the satellite chlorophyll image (10, 21, 25 February and 19, 30 January). The lines represent the trajectory between these dates.

reported in sediments of Taiwan Strait when $1200 \times 10^3 \text{ cells l}^{-1}$ were present in the water column (Liu *et al.*, 2020). A similar ratio between concentrations of cysts and vegetative cell abundances to the nGC has been reported offshore from Rías de Galicia, a maximum concentration of 263 cysts cm^3 wet weight of surface sediments were related to a HAB event that occurred in 2005 with cell abundances that reached $634 \times 10^3 \text{ cells l}^{-1}$ (Figueroa *et al.*, 2008).

The relationship between cyst abundance and vegetative cells will depend on environmental conditions, local strain physiology,

circulation and hydrodynamic processes that affect sediment dynamics. The analysis of the development and dispersion of the 2017 bloom and the dynamics of the cysts between a non-HAB and a HAB year permit us to identify probable critical conditions for the appearance blooms in the region. In 2017, maximum cell abundances were registered in January and gradually decreased to the end of February. HABs in the nGC have a clear seasonality of appearance, *G. catenatum* is detected from November/December and disappears in April/May (Ramírez Castillo, 2020). Relatively low abundances (lower than

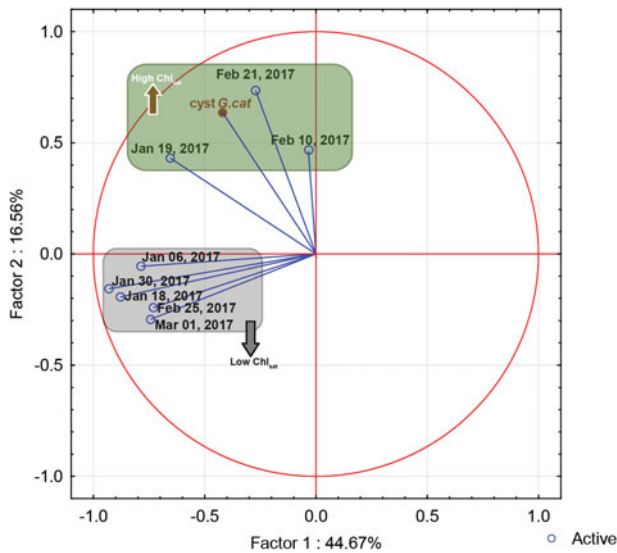


Fig. 6. PCA results of the relation between Chl_{sat} concentration of several days between 19 January, 10 and 21 February with cyst abundance.

$20 \times 10^3 \text{ cells l}^{-1}$) have been detected before 2015. From this time, HABs have been registered every year except for 2016 (Medina-Elizalde, 2021).

Favourable temperatures for vegetative cell growth seem essential for the development of HABs in the nGC. *Gymnodinium catenatum* of the Gulf of California is considered as a warm ecotype (Band-Schmidt *et al.*, 2004). Strains isolated in southern locations (Concepción Bay, La Paz Bay, Mazatlán Bay) grow in a wide temperature interval from 15–29 °C but have maximum growth rates between 21–29 °C (Band-Schmidt *et al.*, 2004). Also, blooms in the south-east coast of the GC and in the tropical Pacific coast of Mexico occur in summer after upwelling events (Band-Schmidt *et al.*, 2004, 2010; Morquecho & Lechuga, 2004; Gárate-Lizárraga *et al.*, 2007a). Blooms of *G. catenatum* in the nGC occur in winter when temperature drops below 17–18 °C and they are not registered in warmer months (Medina-Elizalde *et al.*, 2018; Ramírez Castillo, 2020; Medina-Elizalde, 2021). This species proliferated at temperatures as low as 13–14 °C (Ramírez Castillo, 2020). Therefore, *G. catenatum* of this region can be characterized as a cold ecotype since it presents similar temperature preferences as the ones reported in Tasmania (Blackburn *et al.*, 1989; Hallegraeff *et al.*, 1995).

The proliferation of this species probably does not depend on a pulsed input of nutrients associated with upwellings. We did not measure the concentration of nutrients, but it is well known that nutrient concentrations are high in the nGC. Mixing by tidal currents and winds, sediment re-suspension, remineralization in the wetlands from the Colorado River delta maintain a constant high macronutrient concentration in this region (Millán-Núñez *et al.*, 1999; Orozco *et al.*, 2015; Ramírez-León *et al.*, 2015).

Another key observation that HABs do not depend on pulsed inputs of nutrient is that the high phytoplankton biomass accumulation initiated in the west coast and dispersed westward and northward covering almost the entire region ~1 month after its initiation. This dispersion pattern seems consistent every year since the times of implementation of sanitary bans (closure of extraction areas of bivalves) follow the same pattern (Medina-Elizalde, 2021). Usually, *P. globosa* extraction areas south from San Felipe are the first to be closed during winter (Medina-Elizalde, 2021). There are no punctual sources of organic matter and terrigenous nutrients (there are no river discharges) in this area and upwelling occurs in the continental side of the Gulf of California when winds have a southward direction (Brusca *et al.*, 2017).

We propose that resuspension of cysts, particularly on the west coast, must be another critical process for HAB development in

the nGC. Assuming that the deposition of seedbeds in 2015 was similar to that of February 2017, then localization of seedbeds in July 2016 represents the result of long-term hydrodynamic processes that maintain cysts in the nGC for a period of at least 2 years. Cysts seem to be transported in an eastward direction after deposition and accumulated in an extensive area north of San Felipe that is probably the seedbed responsible for the initiation of HABs in the region.

Cyst distribution in the nGC seems to be a combination of vertical and horizontal advection that also affects sediment transport. The effect of strong semidiurnal tidal currents causes resuspension which is present continuously in the region, mean monthly velocities and their difference between surface and close to the bottom are likely to be responsible for cyst re-distribution. Localization of seedbeds during February 2017 reflects short-term processes between deposition and redistribution of the cyst in sediments. The deposition of cysts was related to the evolution of the HAB after its initiation on the west coast and mild current conditions cause deposition of cysts produced during the HAB. This was confirmed by the particle advection analysis. In contrast, particles were on the continental side of the GC. Then predominant circulation associated with the anticyclonic gyre seems to disperse vegetative cells from the west to the east coast of the nGC coinciding with areas of the predominance of fine sands. Cysts present in front of San Felipe (west coast) originated from the centre of the uGC and the seedbed detected in Adair Bay is likely the result of transportation of cells and cyst deposition related to convergence of strong surface currents present during winter in the area. After deposition, circulation and tidal processes could reduce the concentration of cysts in the original deposition areas, and they could be relocated into other zones.

An autochthonous origin of HABs seems to be the scenario that prevails in the nGC. We demonstrated that the nGC is a retention area of cysts (and sediments) that permit the formation of seedbeds that could be important for *G. catenatum* HAB development. Particularly, the uGC is an area of high particle retention and low reception of particles from other areas (Marinone, 2012) and it has been calculated that particles can travel about 400 km before leaving the area after 30 days (Marinone *et al.*, 2011).

An autochthonous origin of HABs is shared with Tasmania (Hallegraeff *et al.*, 2012) and Concepcion Bay, Baja California Sur (Morquecho & Lechuga-Devéze, 2003, 2004). However, as mentioned previously cyst concentration cannot be related to the magnitude of *G. catenatum* HABs even in these conditions. In contrast, it has been recognized that *A. catenella* cyst concentration in seedbeds seems to determine the intensity of the blooms in the Gulf of Maine (Anderson *et al.*, 2014). Cyst distribution, sediment transport and bloom dynamics of *A. catenella* have been extensively studied and it is recognized that resuspension is main cause of the redistribution of cysts in the Gulf of Maine. Approximately 1 mm of sediment is resuspended and could be transported laterally, modifying the spatial distribution of the cysts, and they would have better access to light, which favours germination and growth (Anderson *et al.*, 2014; Aretxabaleta *et al.*, 2014; Butman *et al.*, 2014). This must occur close to the coast where the semidiurnal tides and costal currents intensify (Butman *et al.*, 2014). The same process may be present in the nGC where the suspended cysts form biogenic conglomerates in the water column together with terrigenous particles of the same size range and are transported to relatively shallow areas. There, the cysts remain until they are resuspended by changes in the direction and intensity of the currents. This occurs during the autumn–winter transition (Montes *et al.*, 2016).

However, physiological differences must be considered when comparing the process of HAB development between *G. catenatum* and *A. catenella*. Resting cyst production rate of *G. catenatum*

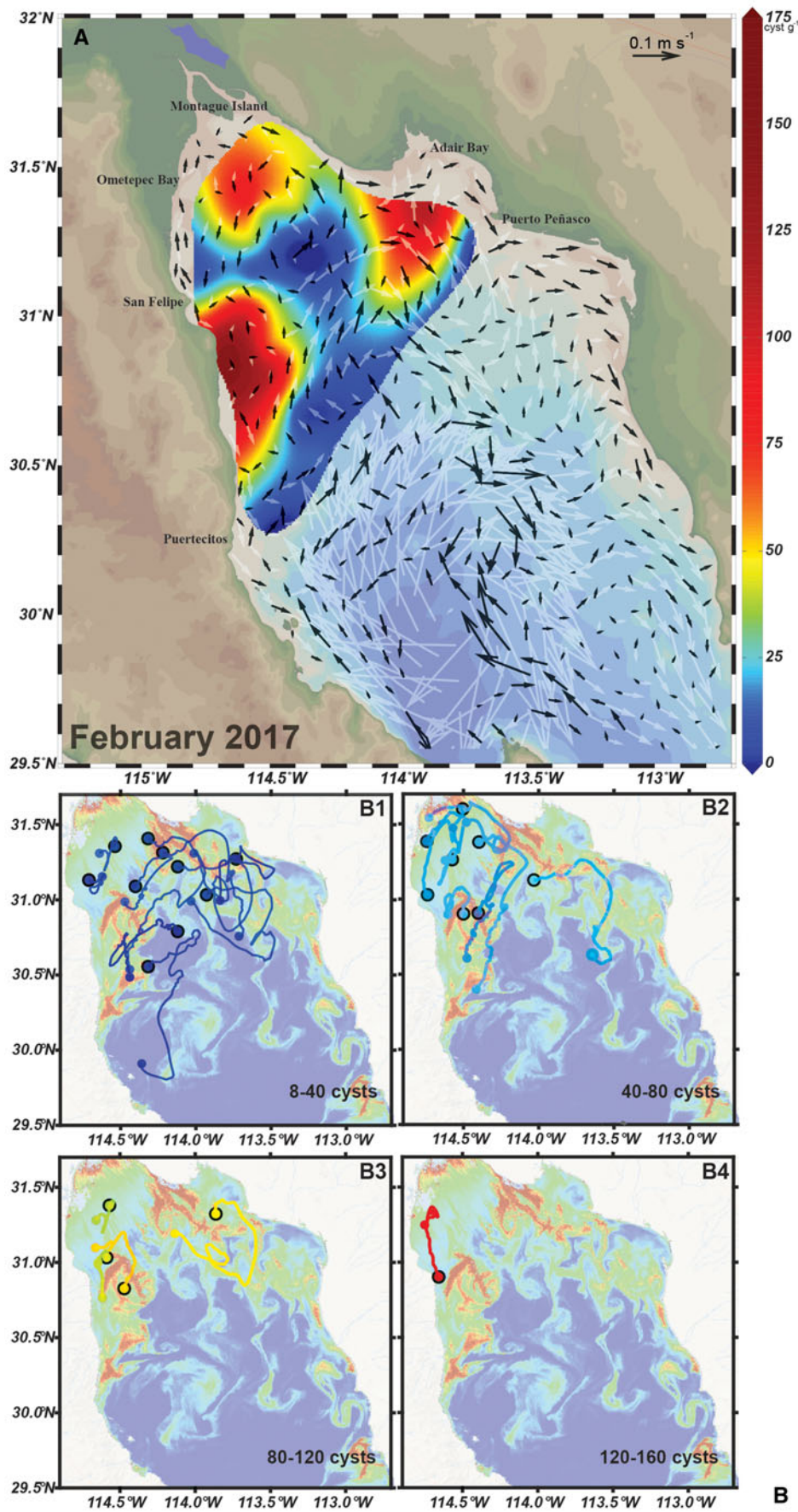


Fig. 7. (A) Vectors of monthly mean velocity at the surface (white vectors) and at 5 metres above the bottom (black vectors), and *G. catenatum* distribution (colour scale) in February 2017; the maximum surface speed is 0.42 m s^{-1} . (B) Lagrangian 22-day trajectories, during 3–25 February 2017; large dots and black outline represent the positions final of the advected particles on 25 February; these final positions correspond to the observational points with non-zero cyst concentration indicated by the rainbow-coloured palette. The trajectories were separated according to their cyst concentration in four ranges for clarity in the plots, and are plotted on the Chl_{sat} image of 10 February 2017, as a base map.

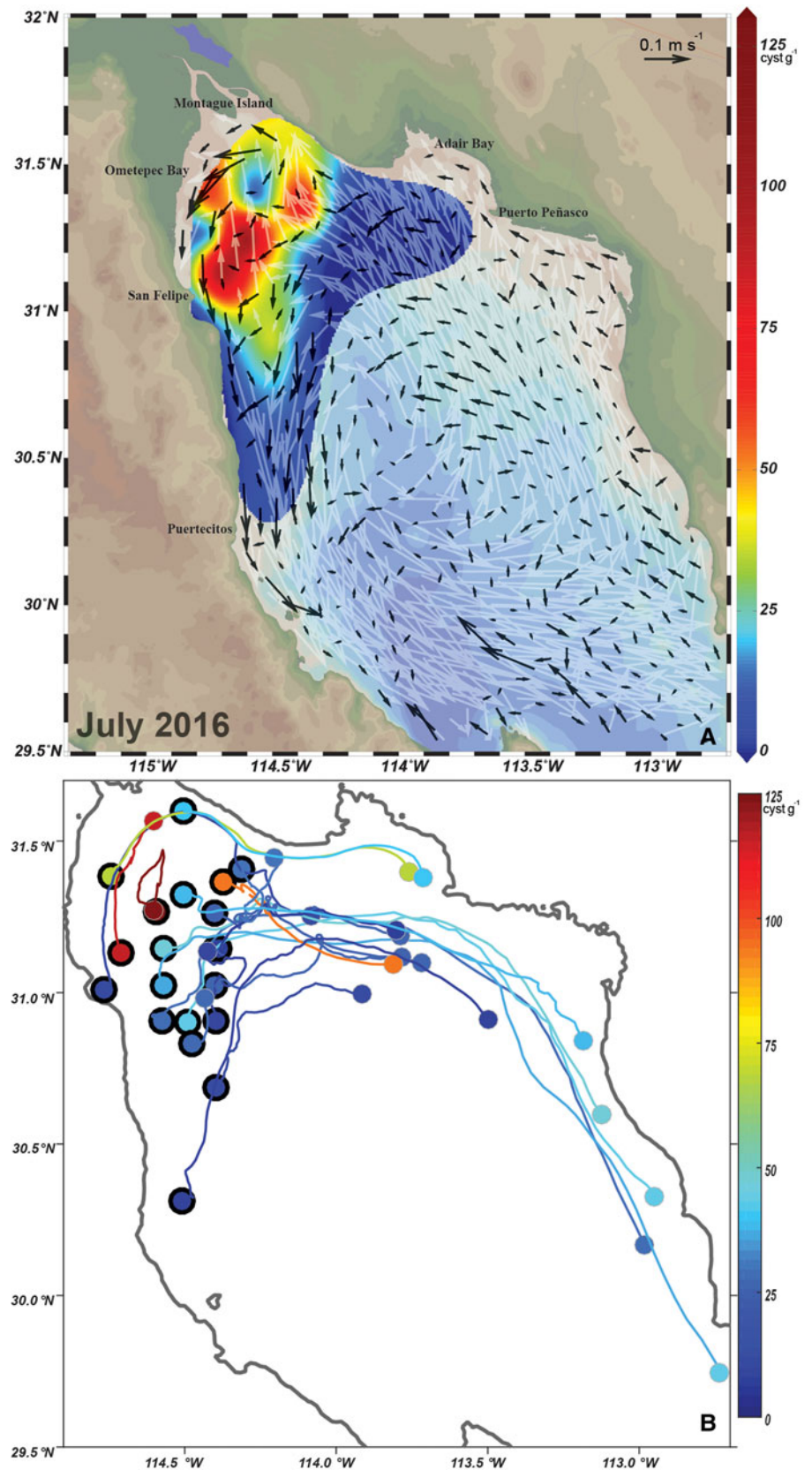


Fig. 8. (A) Vectors of monthly mean velocity at the surface (white vectors) and at 5 m above the bottom (black vectors), and *G. catenatum* distribution (colour) in July 2016; the maximum surface speed 0.54 m s^{-1} . (B) Lagrangian 22-day trajectories, during 1–22 July 2016; large dots and black outline represent the final positions of the advected particles on 22 July; these final positions correspond to the observational points with non-zero cyst concentration indicated by the rainbow-coloured palette.

is between 10–40% of total vegetative cells, and cysts have a dormancy period of 1–2 weeks (Blackburn *et al.*, 1989). In contrast, cyst generation for *A. catenella* could be as high as 100% of vegetative cells and they present a dormancy period of 1–6 months (Figueroa & Bravo, 2005). Therefore, the concentrations of *A. catenella* cysts in the sediment are much higher than the ones reported for *G. catenatum*. HABs of *A. catenella* probably

depend on a large inoculum of vegetative cells associated with cyst germination while *G. catenatum* proliferation probably relies more on vegetative growth after cyst germination.

The role of seedbeds on *G. catenatum* HABs and its importance in HAB development still is an open field of investigation. Most of the studies report concentrations from limited sampling points. This is the only work that describes the presence of

extensive defined areas of high accumulation of cysts of this species. Having the opportunity to compare the concentration and spatial distribution of cysts between a HAB and a non-HAB year permitted us to investigate the dynamic nature of seedbeds and the behaviour of cysts as sedimentary particles in the nGC. The redistribution and retention of these particles in the zone must be crucial for HAB formation in the nGC.

Supplementary material. The supplementary material for this article can be found at <https://doi.org/10.1017/S0025315421000795>

Acknowledgements. We thank Oc. Edna Collins for the support in palynological analysis. We also thank CONACYT for financial support of the PhD scholarship 24805 – CV617226.

Financial support. This work was funded by CONACYT scholarship 24805 – CV617226; FORDECYT – CONACYT project number 260040-2015. D. Rivas was supported by CICESE through the internal project 625118. The GODAS and NARR products were provided by the National Oceanic and Atmospheric Administration (NOAA) – Earth System Research Laboratory (ESRL) Physical Science Division (PSD) through its website: <http://www.esrl.noaa.gov/psd/data/gridded/>. The altimeter product was provided by the Archiving, Validation, and Interpretation of Satellite Oceanographic data (AVISO) through its website (<https://www.aviso.altimetry.fr>). The satellite SST imagery was available at the National Aeronautics and Space Administration (NASA) OceanColor Web: <http://oceancolor.gsfc.nasa.gov>.

References

- Álvarez-Borrego S, Flores-Baéz BP and Galindo-Bect LA (1975) Hidrología del Alto Golfo de California II. Condiciones durante invierno, primavera y verano. *Ciencias Marinas* 2, 21–36.
- Amorim A and Dale B (1998) Distribution of cysts from toxic or potentially toxic dinoflagellates along the Portuguese coast. In Reguera B, Blanco J, Fernandez M and Wyatt T (eds), *Harmful Algae, Proceedings of the VIII International Conference on Harmful Algae*. Santiago de Compostela: Xunta de Galicia and Intergovernmental Oceanographic Commission of UNESCO, pp. 64–65.
- Amorim A, Dale B, Godinho R and Brotas V (2001) *Gymnodinium catenatum*-like cysts (Dinophyceae) in recent sediments from the coast of Portugal. *Phycologia* 40, 572–582.
- Anderson DM, Jacobson DM, Bravo I and Wrenn JH (1988) The unique, microreticulate cyst of the naked dinoflagellate *Gymnodinium catenatum*. *Journal of Phycology* 24, 255–262.
- Anderson DM, Stock CA, Keafer BA, Nelson AB, Thompson B, McGillicuddy Jr DJ, Keller M, Matrai PA and Martin J (2005) *Alexandrium fundyense* cyst dynamics in the Gulf of Maine. *Deep Sea Research Part II: Topical Studies in Oceanography* 52, 2522–2542.
- Anderson DM, Keafer BA, Kleindinst JL, McGillicuddy DJ Jr, Martin JL, Norton K, Pilskaln CH, Smith JL, Sherwood CR and Butman B (2014) *Alexandrium fundyense* cysts in the Gulf of Maine: long-term time series of abundance and distribution, and linkages to past and future blooms. *Deep Sea Research Part II: Topical Studies in Oceanography* 103, 6–26.
- Aretxabaleta AL, Butman B, Signell RP, Dalyander PS, Sherwood CR, Sheremet VA and McGillicuddy DJ Jr (2014) Near-bottom circulation and dispersion of sediment containing *Alexandrium fundyense* cysts in the Gulf of Maine during 2010–2011. *Deep Sea Research Part II: Topical Studies in Oceanography* 103, 96–111.
- Argote ML, Amador A, Lavín MF and Hunter JR (1995) Tidal dissipation and stratification in the Gulf of California. *Journal of Geophysical Research: Oceans* (1978–2012) 100, 16103–16118.
- Band-Schmidt CJ, Morquecho L, Lechuga-Devéze CH and Anderson DM (2004) Effects of growth medium, temperature, salinity and seawater source on the growth of *Gymnodinium catenatum* (Dinophyceae) from Bahía Concepción, Gulf of California, México. *Journal of Plankton Research* 26, 1459–1470.
- Band-Schmidt CJ, Bustillos-Guzmán J, Gárate-Lizárraga I, Lechuga-Devéze CH, Reinhardt K and Luckas B (2005) Paralytic shellfish toxin profile in strains of the dinoflagellate *Gymnodinium catenatum* Graham and the scallop *Argopecten ventricosus* GB Sowerby II from Bahía Concepción, Gulf of California, Mexico. *Harmful Algae* 4, 21–31.
- Band-Schmidt CJ, Bustillos-Guzmán JJ, López-Cortés DJ, Gárate-Lizárraga I, Núñez-Vázquez EJ and Hernández-Sandoval FE (2010) Ecological and physiological studies of *Gymnodinium catenatum* in the Mexican Pacific: a review. *Marine Drugs* 8, 1935–1961.
- Band-Schmidt CJ, Duran-Riveroll LM, Bustillos-Guzmán JJ, Leyva-Valencia I, Lopez-Cortés DJ, Nuñez-Vázquez EJ, Hernández-Sandoval FE, Ramirez-Rodriguez DV (2019) Paralytic toxin producing dinoflagellates in Latin America: ecology and physiology (a review). *Frontiers in Marine Science* 6, 42.
- Beier E and Ripa P (1999) Seasonal gyres in the northern Gulf of California. *Journal of Physical Oceanography* 29, 305–311.
- Benninghoff WS (1962) Calculations of pollen and spore density in sediments by addition of exotic pollen in known quantities. *Pollen Spores* 4, 332.
- Blackburn SI, Hallegraeff GM and Bolch CJ (1989) Vegetative reproduction and sexual life cycle of the toxic dinoflagellate *Gymnodinium catenatum* from Tasmania, Australia. *Journal of Phycology* 25, 577–590.
- Blanco J (1995) The distribution of dinoflagellate cysts along the Galician (NW Spain) coast. *Journal of Plankton Research* 17, 283–302.
- Blott S and Pye K (2001) Gradistat: a grain size distribution and statistic package for the analysis of unconsolidated sediments. *Earth Surface Processes and Landforms* 26, 1237–1248.
- Bolch CJ and Hallegraeff GM (1990) Dinoflagellate cysts in recent marine sediments from Tasmania, Australia. *Botanica Marina* 33, 173–192.
- Bolch CJ, Negri AP and Hallegraeff GM (1999) *Gymnodinium microreticulatum* sp. nov. (Dinophyceae): a naked, microreticulate cyst-producing dinoflagellate, distinct from *Gymnodinium catenatum* and *Gymnodinium nolleri*. *Phycologia* 38, 301–313.
- Bray NA and Robles JM (1991) Physical oceanography of the Gulf of California. Chapter 25: Part V. Physical Oceanography, Primary Productivity, Sedimentology. In The Gulf and Peninsular Province of the Californias, *Memoir of the American association of Petroleum Geologists*, 47, 511–553.
- Brusca RC, Álvarez-Borrego S, Hastings PA and Findley LT (2017) Colorado River flow and biological productivity in the northern Gulf of California, México. *Earth-Science Reviews* 164, 1–30.
- Butman B, Aretxabaleta AL, Dickhudt PJ, Dalyander PS, Sherwood CR, Anderson DM, Keafer BA and Signell RP (2014) Investigating the importance of sediment resuspension in *Alexandrium fundyense* cyst population dynamics in the Gulf of Maine. *Deep Sea Research Part II: Topical Studies in Oceanography* 103, 79–95.
- Carriquiry JD, Sánchez A and Camacho-Ibar VF (2001) Sedimentation in the northern Gulf of California after cessation of the Colorado river discharge. *Sedimentary Geology* 144, 37–62.
- Cochran WG (1963) *Sampling Techniques*, 2nd Edn. New York, NY: John Wiley & Sons.
- COFEPRIS (2015) Comisión Federal para la Protección contra Riesgos Sanitarios. Presencia de marea roja en México durante 2015. Secretaría de Salud. Available at <http://www.cofepris.gob.mx/> (Accessed online 29 January 2021).
- Cruz-Rico J and Rivas D (2018) Physical and biogeochemical variability in Todos Santos Bay, northwestern Baja California, derived from a numerical NPZD model. *Journal of Marine Systems* 183, 63–75.
- Dale B (1983) Dinoflagellate resting cysts: benthic plankton. In Fryxell GA (ed.), *Survival Strategies of the Algae*. Cambridge: Cambridge University Press, pp. 69–136.
- Duque-Herrera AF, Helenes J, Flores-Trujillo JG, Ruiz-Fernández AC and Sánchez-Cabeza JA (2020) Dinoflagellate cysts and ENSO-PDO climate forcing in the southern Gulf of California. *Palaeogeography, Palaeoclimatology, Palaeoecology* 560, 110055.
- Erdner DL, Percy L, Keafer B, Lewis J and Anderson DM (2010) A quantitative real-time PCR assay for the identification and enumeration of *Alexandrium* cysts in marine sediments. *Deep Sea Research Part II: Topical Studies in Oceanography* 57, 279–287.
- Espinosa-Carreón TL and Valdez-Holguín E (2007) Variabilidad interanual de clorofila en el Golfo de California. *Ecología Aplicada* 6, 83–92.
- Fairall CW, Bradley EF, Rogers DP, Edson JB and Young GS (1996) Bulk parameterization of air-sea fluxes for tropical ocean global atmosphere coupled-ocean atmosphere response experiment. *Journal of Geophysical Research: Oceans* 101, 3747–3764.
- Figuerola RI and Bravo I (2005) Sexual reproduction and two different encystment strategies of *Lingulodinium polyedrum* (Dinophyceae) in culture. *Journal of Phycology* 41, 370–379.

- Figueroa RI, Bravo I and Garcés E** (2005) Effects of nutritional factors and different parental crosses on the encystment and excystment of *Alexandrium catenella* (Dinophyceae) in culture. *Phycologia* **44**, 658–670.
- Figueroa RI, Bravo I, Ramilo I, Pazos Y and Moroño A** (2008) New life-cycle stages of *Gymnodinium catenatum* (Dinophyceae): laboratory and field observations. *Aquatic Microbial Ecology* **52**, 13–23.
- Gárate-Lizárraga I, Band-Schmidt CJ, López-Cortés DJ, Bustillos-Guzmán JJ and Erler K** (2007a) Bloom of *Pseudo-nitzschia fraudulenta* in Bahía de La Paz, Gulf of California (June–July 2006). *Harmful Algae News* **33**, 6–7.
- Gárate-Lizárraga I, Arellano-Martínez M, Ceballos-Vázquez BP, Bustillos-Guzmán JJ, López-Cortés DJ and Hernández-Sandoval F** (2007b) Fitoplancton tóxico y presencia de toxinas paralizantes en la almeja mano de león (*Nodipecten subnodosus*, Sowerby, 1835) en la Bahía de Los Ángeles, B.C. In *Resúmenes del II Taller sobre Florecimientos Algales Nocivos, Ensenada, México, 21–23 Noviembre*. Ensenada: CICESE-CETMAR, p. 20.
- Graham HW** (1943) *Gymnodinium catenatum*, a new dinoflagellate from the Gulf of California. *Transactions of the American Microscopical Society* **62**, 259–261.
- Hallegraeff GM, McCausland MA and Brown RK** (1995) Early warning of toxic dinoflagellate blooms of *Gymnodinium catenatum* in southern Tasmanian waters. *Journal of Plankton Research* **17**, 1163–1176.
- Hallegraeff GM, Blackburn SI, Doblín MA and Bolch CJS** (2012) Global toxicology, ecophysiology and population relationships of the chainforming PST dinoflagellate *Gymnodinium catenatum*. *Harmful Algae* **14**, 130–143.
- Hammer Ø, Harper DAT and Ryan PD** (2001) PAST: paleontological statistics software package for education and data analysis. *Palaeontologia Electronica* **4**, 9.
- Harland R, Nordberg K and Filipsson H** (2004) The seasonal occurrence of dinoflagellate cysts in surface sediments from Koljö Fjord, west coast of Sweden – a note. *Review of Palaeobotany and Palynology* **128**, 107–117.
- Horner RA, Greengrove CL, Davies-Vollum KS, Gawel JE, Postel JR and Cox AM** (2011) Spatial distribution of benthic cysts of *Alexandrium catenella* in surface sediments of Puget Sound, Washington, USA. *Harmful Algae* **11**, 96–105.
- Hwang CH, Kim KY, Lee Y and Kim CH** (2011) Spatial distribution of dinoflagellate resting cysts in Yellow Sea surface sediments. *Algae* **26**, 41–50.
- Lavín MF, Durazo R, Palacios E, Argote ML and Carrillo L** (1997) Lagrangian observations of the circulation in the northern Gulf of California. *Journal of Physical Oceanography* **27**, 2298–2305.
- Lavín MF, Godínez VM and Alvarez LG** (1998) Inverse-estuarine features of the upper Gulf of California. *Estuarine, Coastal and Shelf Science* **47**, 769–795.
- Liu D, Shi Y, Di B, Sun Q, Wang Y, Dong Z and Shao H** (2012) The impact of different pollution sources on modern dinoflagellate cysts in Sishili Bay, Yellow Sea, China. *Marine Micropaleontology* **84**, 1–13.
- Liu M, Gu H, Krock B, Luo Z and Zhang Y** (2020) Toxic dinoflagellate blooms of *Gymnodinium catenatum* and their cysts in Taiwan Strait and their relationship to global populations. *Harmful Algae* **97**, 101868.
- López-Cortés DJ, Hernández-Sandoval FE, Band-Schmidt CJ, Bustillos-Guzmán JJ and Núñez-Vázquez EJ** (2016) Condiciones ambientales asociadas a florecimientos algales nocivos en el Golfo de California. In García-Mendoza E, Quijano-Scheggia SI, Olivos-Ortiz A and Núñez-Vázquez EJ (eds), *Florecimientos Algales Nocivos en México*. CICESE: Ensenada, México, p. 438.
- MacKenzie AL** (2014) The risk to New Zealand shellfish aquaculture from paralytic shellfish poisoning (PSP) toxins. *New Zealand Journal of Marine and Freshwater Research* **48**, 430–465.
- Maher LJ Jr.** (1981) Statistics for microfossil concentration measurements employing samples spiked with marker grains. *Review of Palaeobotany and Palynology* **32**, 153–191.
- Marinone SG** (2012) Seasonal surface connectivity in the Gulf of California. *Estuarine, Coastal and Shelf Science* **100**, 133–141.
- Marinone SG, Lavín MF and Parés-Sierra A** (2011) A quantitative characterization of the seasonal Lagrangian circulation of the Gulf of California from a three-dimensional numerical model. *Continental Shelf Research* **31**, 1420–1426.
- Medina-Elizalde J** (2021) Effects of Paralytic Shellfish Toxins on marine mammals, seabirds and geoduck fisheries in the Northern Gulf of California during 2015–2019. PhD thesis. Centro de Investigación Científica y de Educación de Ensenada, Baja California, México, 83 pp.
- Medina-Elizalde J, García-Mendoza E, Turner AD, Sánchez-Bravo YA and Murillo Martínez R** (2018) Transformation and depuration of paralytic shellfish toxins in the geoduck clam *Panopea globosa* from the northern Gulf of California. *Frontiers in Marine Science* **5**, 335.
- Mee LD, Espinosa M and Diaz G** (1986) Paralytic shellfish poisoning with a *Gymnodinium catenatum* red tide on the Pacific coast of Mexico. *Marine Environmental Research* **19**, 77–92.
- Mertens KN, Verhoeven K, Verleye T, Louwey S, Amorim A, Ribeiro S, Deaf AS, Harding IC, De Schepper S, Gonzáles C, Kodrans-Nsiah M, De Vernal A, Henry M, Radi T, Dybkjaer K, Poulsen NE, Feist-Burkhardt S, Chitolie J, Heilmann-Clausen C, Londeix I, Turon J-L, Marret F, Matthiesen J, McCarthy FMG, Prasad V, Pospelova V, Kyffin Hughes JE, Riding JB, Rochon, A, Sangiorgi F, Welters N, Sinclair N, Thun C, Soliman A, Van Nieuwenhove N, Vink A and Young M** (2009) Determining the absolute abundance of dinoflagellate cysts in recent marine sediments: the *Lycopodium* marker-grain method put to the test. *Review of Palaeobotany and Palynology* **157**, 238–252.
- Mertens KN, Price AM and Pospelova V** (2012) Determining the absolute abundance of dinoflagellate cysts in recent marine sediments II: further tests of the *Lycopodium* marker-grain method. *Review of Palaeobotany and Palynology* **184**, 74–81.
- Mesinger F, DiMego G, Kalnay E, Mitchell K, Shafran PC, Ebisuzaki W, Jovic D, Woollen J, Rogers E, Berbery EH, Ek MB, Fan Y, Grumbine R, Higgins W, Li H, Lin Y, Manikin G, Parrish D and Shi W** (2006) North American regional reanalysis. *Bulletin of the American Meteorological Society* **87**, 343–360.
- Millán-Núñez R, Santamaría del Ángel E, Cajal-Medrano R and Barocio-León OA** (1999) The Colorado river Delta: a high primary productivity ecosystem. *Ciencias Marinas* **25**, 509–524.
- Montes JM, Lavín MF and Parés-Sierra AF** (2016) Seasonal heat and salt balance in the upper Gulf of California. *Journal of Coastal Research* **32**, 853–862.
- Morquecho L and Lechuga-Devéze CH** (2003) Dinoflagellate cysts in recent sediments from Bahía Concepción, Gulf of California. *Botanica Marina* **46**, 132–141.
- Morquecho L and Lechuga-Devéze CH** (2004) Seasonal occurrence of planktonic dinoflagellates and cyst production in relationship to environmental variables in subtropical Bahía Concepción, Gulf of California. *Botanica Marina* **47**, 313–322.
- Nehring S** (1994) Spatial distribution of dinoflagellate resting cysts in recent sediments of Kiel Bight, Germany (Baltic Sea). *Ophelia* **39**, 137–158.
- Orozco-Durán A, Daesslé LW, Camacho-Ibar VF, Ortiz-Campos E and Barth JAC** (2015) Turnover and release of P-, N-, Si-nutrients in the Mexicali Valley (Mexico): interactions between the lower Colorado River and adjacent ground-and surface water systems. *Science of the Total Environment* **512**, 185–193.
- Palacios-Hernández E, Beier E, Lavín MF and Ripa P** (2002) The effect of the seasonal variation of stratification on the circulation of the northern Gulf of California. *Journal of Physical Oceanography* **32**, 705–728.
- Peña-Manjarrez JL, Flores-Trujillo JG and Helenes-Escamilla J** (2016) Quistes de dinoflagelados de pared orgánica en las costas de México. In García-Mendoza E, Quijano-Scheggia SI, Olivos-Ortiz A and Nunez-Vazquez EJ (eds), *Florecimientos Algales Nocivos en México*. Ensenada: CICESE, p. 438.
- Penna A, Perini F, Dell'Aversano C, Capellacci S, Tartaglione L, Giacobbe MG, ... Scardi M** (2015) The sxt gene and paralytic shellfish poisoning toxins as markers for the monitoring of toxic *Alexandrium* species blooms. *Environmental Science & Technology* **49**, 14230–14238.
- Pospelova V and Kim SJ** (2010) Dinoflagellate cysts in recent estuarine sediments from aquaculture sites of southern South Korea. *Marine Micropaleontology* **76**, 37–51.
- Pospelova V, de Vernal A and Pedersen TF** (2008) Distribution of dinoflagellate cysts in surface sediments from the northeastern Pacific Ocean (43–25°N) in relation to sea-surface temperature, salinity, productivity and coastal upwelling. *Marine Micropaleontology* **68**, 21–48.
- Ramírez Castillo AM** (2020) Comunidad fitoplanctónica y presencia de *Gymnodinium catenatum* con relación a la temperatura en la Bahía de San Felipe, Baja California, México, Tesis de Licenciatura. Universidad de Colima, 70 pp.
- Ramírez-León MR, Álvarez-Borrego S, Turrent Thompson C, Gaxiola Castro G and Heckel Dziendzielewski G** (2015) Nutrient input from the Colorado River to the northern Gulf of California is not required to maintain a productive pelagic ecosystem. *Ciencias Marinas* **41**, 169–188.
- Ravichandran M, Behringer D, Sivareddy S, Girishkumar MS, Chacko N and Harikumar R** (2013) Evaluation of the Global Ocean data assimilation system at INCOIS: the tropical Indian ocean. *Ocean Model* **69**, 1–13.

- Rees AJJ and Hallegraeff GM** (1991) Ultrastructure of the toxic dinoflagellate *Gymnodinium catenatum* Graham. *Phycologia* **30**, 90–105.
- Ribeiro S and Amorim A** (2008) Environmental drivers of temporal succession in recent dinoflagellate cyst assemblages from a coastal site in the North-East Atlantic (Lisbon Bay, Portugal). *Marine Micropaleontology* **68**, 156–178.
- Rio MH, Pascual A, Poulain PM, Menna M, Barceló B and Tintoré J** (2014) Computation of a new mean dynamic topography for the Mediterranean Sea from model outputs, altimeter measurements and oceanographic in situ data. *Ocean Science* **10**, 731–744.
- Rivas D and Samelson RM** (2011) A numerical modeling study of the upwelling source waters along the Oregon coast during 2005. *Journal of Physical Oceanography* **41**, 88–112.
- Schlitzer R** (2021) Ocean Data View. <https://odv.awi.de>.
- Shin HH, Yoon YH, Kim YO and Matsuoka K** (2011) Dinoflagellate cysts in surface sediments from southern coast of Korea. *Estuaries and Coasts* **34**, 712–725.
- Siegel S and Castellan NJ** (1988) *Nonparametric Statistics for the Behavioural Sciences*, 2nd Edn. New York, NY: McGraw-Hill Book Company, pp. 144–151.
- Singh AS and Masuku MB** (2013) Fundamentals of applied research and sampling techniques. *International Journal of Medical and Applied Sciences* **2**, 124–132.
- StatSoft, Inc.** (2014) STATISTICA (data analysis software system), version 12. <http://www.statsoft.com/>.
- Stock, G.G.** (1976) Modeling of Tides and Tidal Dissipation in the Gulf of California. PhD dissertation, Scripps Institution of Oceanography, University of California, San Diego, La Jolla, California, 102 pp.
- Tahvanainen P, Alpermann TJ, Figueroa RI, John U, Hakanen P, Nagai S, Blomster J and Kremp A** (2012) Patterns of post-glacial genetic differentiation in marginal populations of a marine microalga. *PLoS ONE* **7**, e53602.
- Triki HZ, Laabir M, Lafabrie C, Malouche D, Bancon-Montigny C, Gonzalez C, Deidun A, Pringault O and Daly-Yahia OK** (2017) Do the levels of industrial pollutants influence the distribution and abundance of dinoflagellate cysts in the recently-deposited sediment of a Mediterranean coastal ecosystem? *Science of the Total Environment* **595**, 380–392.
- Wang Z, Matsuoka K, Qi Y and Chen J** (2004) Dinoflagellate cysts in recent sediments from Chinese coastal waters. *Marine Ecology* **25**, 289–311.
- Wentworth CK** (1922) A scale of grade and class terms for clastic sediments. *Journal of Geology* **30**, 377–392.
- Wiese M, D'agostino PM, Mihali TK, Moffitt MC and Neilan BA** (2010) Neurotoxic alkaloids: saxitoxin and its analogs. *Marine Drugs* **8**, 2185–2211.
- Wood GD, Gabriel AM and Lawson JC** (1996) Palynological techniques-processing and microscopy. In Jasonius J and McGregor DC (eds), *Palynology: Principles and Application*. Dallas: American Association of Stratigraphic Palynologists Foundation, vol. 1, pp. 29–50.